

First principles-based calculation of the electrocaloric effect in BaTiO₃: comparison between direct and indirect methods

Madhura Marathe,^{1,*} Anna Grünebohm,² Takeshi Nishimatsu,³ Peter Entel,² and Claude Ederer^{1,†}

¹*Materials Theory, ETH Zürich, Wolfgang-Pauli-Str. 27, 8093 Zürich, Switzerland*

²*Faculty of Physics and CENIDE, University of Duisburg-Essen, 47048, Duisburg, Germany*

³*Institute for Materials Research, Tohoku University, Sendai 980-8577, Japan*

(Dated: June 2, 2015)

We use molecular dynamics simulations for a first principles-based effective Hamiltonian to calculate two important quantities characterizing the electrocaloric effect in BaTiO₃, the adiabatic temperature change ΔT and the isothermal entropy change ΔS , for different electric field strengths. We compare direct and indirect methods to obtain ΔT and ΔS , and we confirm that both methods indeed lead to identical result provided that the system does not actually undergo a first order phase transition. We also show that a large electrocaloric response is obtained for electric fields beyond the critical field strength for the first order phase transition. Furthermore, our work fills several gaps regarding the application of the first principles-based effective Hamiltonian approach, which represents a very attractive and powerful method for the quantitative prediction of electrocaloric properties. In particular, we discuss the importance of maintaining thermal equilibrium during the field ramping when calculating ΔT using the direct method within a molecular dynamics approach.

I. INTRODUCTION

The ongoing search for alternative cooling technologies which are more energy-efficient and environmentally friendly than conventional vapor-compression refrigerators and offer the additional possibility for device miniaturization has boosted research activities within the fields of electrocaloric, elastocaloric, and magnetocaloric effects.^{1–3} The common feature in all three cases is that the application of an external field (either electric, stress, or magnetic field) under adiabatic conditions, i.e. when the active material is thermally isolated from the environment, results in a temperature change of the corresponding material. This reversible temperature change can be used to transfer heat from a cool reservoir (the heat load) to a warmer reservoir (e.g. the environment), thereby lowering the temperature of the heat load (or keeping it at constant low temperature). It has been found that such caloric effects are especially large close to ferroic first order phase transitions, where giant responses can be triggered through relatively modest fields.^{1–3}

In particular the electrocaloric (EC) effect has become very attractive for potential future applications, due to the discovery of a giant EC temperature change of 12 K in Pb(Zr,Ti)O₃ thin films.⁴ Here, the high crystalline quality that can be achieved in thin film samples allows the application of rather high electric fields without triggering a dielectric breakdown of the samples. In recent years, a large number of studies – both theoretical and experimental – have contributed to a better understanding of the EC effect (see, e.g. Refs. 5–7 and references therein).

Nevertheless, direct measurements of the adiabatic temperature change are still rather challenging, in particular for the case of thin film samples. Therefore, an indirect determination of this temperature change is often preferred. The indirect method is based on a ther-

modynamic Maxwell relation connecting the isothermal field-induced entropy change with the temperature dependence of the electric polarization at fixed electric field:

$$\left(\frac{\partial S}{\partial \mathcal{E}}\right)\Big|_T = \left(\frac{\partial P}{\partial T}\right)\Big|_{\mathcal{E}}. \quad (1)$$

The adiabatic temperature change ΔT can then be obtained from pyroelectric measurements, i.e. by measuring the electric polarization P as function of temperature T at different electric fields \mathcal{E} :

$$\Delta T = - \int_{\mathcal{E}_1}^{\mathcal{E}_2} \frac{T}{C_{p,\mathcal{E}}} \left(\frac{\partial P}{\partial T}\right)\Big|_{\mathcal{E}} d\mathcal{E}. \quad (2)$$

Here, $C_{p,\mathcal{E}}$ is the specific heat at constant pressure and applied field, and the external field is varied from \mathcal{E}_1 to \mathcal{E}_2 . It has to be noted that, if the system undergoes a first order phase transition, the derivative $\partial P/\partial T$ is ill-defined and the specific heat diverges, which in principle does not allow application of Eq. (2). Furthermore, a possible contribution to the EC effect stemming from the latent heat of the first order phase transition is not accounted for by Eq. (2). Instead, the Clausius-Clapeyron equation has to be used to obtain the corresponding contribution. In addition, the indirect method is only suitable for ergodic systems. For example, it was shown that the results from direct and indirect measurements do not match for relaxor polymers,⁸ but compare well for “normal” ferroelectric polymers,⁹ Finally, the influence of domains and anisotropy effects are not covered by the scalar form of the Maxwell relation, Eq. (1).¹⁰

Another important quantity for characterizing the EC effect is the isothermal entropy change ΔS , which is related to the amount of heat that is required to keep the system at constant temperature while an electric field is applied or removed. The isothermal entropy change can also be obtained indirectly from pyroelectric measure-

ments by simply integrating Eq. (1):

$$\Delta S = \int_{\mathcal{E}_1}^{\mathcal{E}_2} \left(\frac{\partial P}{\partial T} \right) \Big|_{\mathcal{E}} d\mathcal{E}. \quad (3)$$

On the other hand, ΔS can also be obtained in a (quasi-) direct way from integrating the specific heat at constant electric field:

$$\Delta S = \int_{T_1}^T \frac{C_{p,\mathcal{E}_1} - C_{p,\mathcal{E}_2}}{T'} dT'. \quad (4)$$

Note that strictly speaking this relation is only valid for $T_1 \rightarrow 0$. Nevertheless, for sufficiently low T_1 one can assume that $S(T_1, \mathcal{E}_1) \approx S(T_1, \mathcal{E}_2)$ and then Eq. (4) can be expected to give a good estimate of ΔS .^{3,11}

In the work presented in this article, we use a first principles-based effective Hamiltonian approach¹²⁻¹⁴ to calculate the EC effect in the prototypical ferroelectric perovskite BaTiO₃, and to address the applicability of the indirect method for evaluating ΔT and ΔS . Performing micro-canonical molecular dynamics (MD) on the effective Hamiltonian allows for a direct calculation of the EC temperature change under application or removal of an electric field. Within the same framework, the temperature dependence of the electric polarization under different electric fields can be calculated and the temperature and entropy changes can then be evaluated via Eqs. (2) and (3). Thus, the effective Hamiltonian provides a simplified but nevertheless realistic “testing ground” for the general applicability of the indirect methods.

Previous studies employing first principles-based effective Hamiltonians have found good agreement between direct and indirect calculations of the EC temperature change,^{15,16} provided that both \mathcal{E}_1 and \mathcal{E}_2 are above the critical field for the first order phase transition, i.e. in a regime where no discontinuities of the polarization occur as function of temperature and electric field. In Ref. 15 the EC temperature change for Ba_{0.5}Sr_{0.5}TiO₃ has been calculated using micro-canonical Monte Carlo simulations (Creutz algorithm), and the so-obtained values have been compared with the indirect evaluation based on Eq. (2), where $P(T, \mathcal{E})$ has been obtained from standard Monte Carlo simulations within the canonical ensemble. In Ref. 16, the direct calculation of ΔT for BaTiO₃ has been performed using a micro-canonical MD algorithm. The indirect evaluation of ΔT using Eq. (2) showed reasonable agreement with the corresponding directly calculated values. Discrepancies were attributed to inconsistencies arising from an empirical, temperature-dependent, pressure correction and to the use of a constant empirical value for the specific heat (the experimental value for $C_{p,\mathcal{E}}$ at room temperature was used in Ref. 16). It is important to note that $C_{p,\mathcal{E}}$ is not constant and varies significantly with temperature and applied field, especially near the phase transition.¹⁷

Here, we calculate the specific heat of the effective Hamiltonian, as function of temperature and electric field, in order to allow for a fully consistent comparison between the direct and indirect evaluation of ΔT

and ΔS . We confirm that both methods indeed lead to identical result provided that the system does not actually undergo a first order phase transition. We also show that the actual transition is not crucial for obtaining a sizable EC response and compare this with the case of magnetocaloric Heusler alloys. Furthermore, we calculate the isothermal EC entropy change and again demonstrate good agreement between direct and indirect methods. Finally, we investigate how fast the electric field can be changed within the MD simulation without the system going out of thermal equilibrium. In particular, we demonstrate the importance of maintaining equilibrium during the simulation by monitoring changes in the total energy of the system.

This paper is organized as follows. In Section II, we briefly describe our computational method. Our results are then presented in Section III, which is divided into two parts, the first describing the effect of different ramping rates for the electric field, the second discussing the EC temperature and entropy changes. Finally, in the last section, we summarize our main results and conclusions.

II. COMPUTATIONAL METHOD

For our study, we use the effective Hamiltonian proposed by Zhong *et al.*^{12,13} This effective Hamiltonian is applicable to ferroelectrics with a cubic perovskite parent structure. The ferroelectric polarization in these materials can be described by a relative displacement of cations and anions, represented by a soft mode variable in the Hamiltonian. In addition, local strain variables are included. This type of description retains the dominant terms in the total energy while reducing the number of degrees of freedom per unit cell from 15 to 6 (3 soft mode variables and 3 local strain variables).

All parameters for the effective Hamiltonian can be obtained using *ab initio* density functional theory calculations.^{13,18} The effective Hamiltonian approach is therefore able to determine temperature-dependent properties of ferroelectric materials without the need for empirical input parameters. For example, it was demonstrated that the three consecutive phase transitions in bulk BaTiO₃ are successfully reproduced.¹² Furthermore, the effective Hamiltonian approach has been used successfully for the calculation of EC properties.^{15,16,19-22}

We perform MD simulations employing the effective Hamiltonian as implemented in the feram code¹⁴ (<http://loto.sourceforge.net/feram/>), using the available parameter set for BaTiO₃,¹⁸ which has been obtained using the generalized gradient approximation for the exchange-correlation functional according to Wu and Cohen.²³

In order to *directly* calculate the adiabatic EC temperature change, we first thermalize the system at a given temperature and electric field using a Nosé-Poincaré thermostat.²⁴ We then switch off the thermostat, i.e. we switch to the micro-canonical ensemble, and slowly

change the electric field while monitoring the resulting changes in the total and kinetic energies. These calculations are performed using a $96 \times 96 \times 96$ supercell, i.e. corresponding to 96 simple perovskite unit cells along each cartesian direction. A time step of 1 fs per MD step is used and the thermalization (averaging) time for these direct calculations is equal to 80 ps (40 ps). As usual, the temperature is calculated from the kinetic energy, E_{kin} , of the system:

$$T = \frac{2E_{\text{kin}}}{N_f k_B}, \quad (5)$$

where N_f denotes the number of degrees of freedom of the system and k_B is the Boltzmann constant. The EC temperature change ΔT is then simply obtained from the difference between the initial and final temperature of the system, i.e. before and after the electric field is ramped on or off.

To reduce the computational effort, we use a simplified treatment for the local strain variables, which are obtained by minimization of the total energy for the current soft-mode configuration in each MD step. Thus, our model contains only $N_f = 3$ dynamic degrees of freedom per unit cell (the 3 soft mode variables), compared to the original 15. As a result, the model specific heat and the directly calculated ΔT need to be rescaled before comparing to experimental data.¹⁶ However, since the focus of this work is on the internal consistency within the model description, in order to assess the general validity of the indirect determination of ΔT and ΔS , and not on a quantitative comparison with experimental data, we do not perform such rescaling within this work, i.e. except where otherwise noted, all presented values for ΔT and $C_{p,\varepsilon}$ refer to the model system and not to the real material. We also note that a simple rescaling of ΔT neglects the fact that the simulation corresponds to a “wrong” final state of the system, i.e. with different temperature and polarization compared to the final state that would be obtained in a real experiment, and therefore corrects only partially for the missing degrees of freedom.

To calculate the adiabatic temperature change and the isothermal entropy change using the *indirect* method, we calculate polarization as function of temperature (on a 1 K grid) at several applied electric fields using a $16 \times 16 \times 16$ simulation cell, a thermalization time of 120 ps and an averaging time of 80 ps, with a 2 fs time step per MD iteration. These calculations are performed in the canonical ensemble using the Nosé-Poincaré thermostat. We then use smoothing cubic spline functions to fit the polarization versus temperature data, in order to determine $(\partial P/\partial T)_\varepsilon$.

The specific heat of the model Hamiltonian at constant pressure and electric field, required for the indirect calculation of ΔT and the (quasi-) direct calculation of ΔS , is determined by calculating the derivative of the total energy, i.e. by using the relation $C_{p,\varepsilon} = (\partial E_{\text{tot}}/\partial T)_{p,\varepsilon}$, which is applicable for our simulations performed at zero pressure. To calculate $E_{\text{tot}}(T)$, we use a $96 \times 96 \times 96$ sim-

ulation cell, equilibration and averaging times of 80 ps and 40 ps, respectively, and a 2 fs time step. The temperature dependence of $C_{p,\varepsilon}$ has been calculated using “cooling” as well as “heating” simulations, i.e. where the system at a particular temperature is initialized from a thermalized configuration at slightly higher or lower temperature, respectively (see, e.g. Ref. 14). While an appreciable thermal hysteresis is obtained for zero electric field, the thermal hysteresis completely vanishes for fields above 20-30 kV/cm. Therefore, only results from “cooling” runs are presented in the following. In the vicinity of the phase transition, due to the sharp features in $C_{p,\varepsilon}$, a dense 1 K mesh and extended equilibration time is used for field strengths below 75 kV/cm. Otherwise, a temperature grid of 5 K is used and the specific heat is extrapolated to a 1 K temperature grid and a moving average is used to further smooth the data. Above 450 K and for field strengths of more than 200 kV/cm, the total energy varies only weakly. Therefore, we have used a coarser temperature grid of 10 K in that region.

Using $(\partial P/\partial T)_\varepsilon$ and the calculated $C_{p,\varepsilon}$, we can then obtain ΔT from Eq. (2) and ΔS from Eq. (4). We note that we have confirmed the absence of noticeable finite size effect in our results for electric fields above ~ 25 kV/cm, which is above the critical field for the first order phase transition. Therefore, using $(\partial P/\partial T)_\varepsilon$ and $C_{p,\varepsilon}$ obtained from different sizes of the simulation cell does not introduce any significant errors or inconsistencies to our analysis.

In addition, we have performed test calculations assessing the effect of different field ramping rates (see Sec. III A). These tests are performed using a $48 \times 48 \times 48$ simulation cell and a time step of 1 fs. Different thermalization and averaging times have been used in these calculations, depending on the specific field strength, ramping rate, and temperature. In all cases we verified that the system is sufficiently equilibrated and averages were obtained with good accuracy.

We note that in our calculations, we do not apply any empirical pressure corrections, which have been used in previous studies to correct for deficiencies of the first principles calculations or to mimic thermal expansion. Such pressure corrections can lead to better agreement between the calculated and measured transition temperatures.¹⁸ However, as already pointed out in Ref. 16, a temperature-dependent pressure correction can also lead to inconsistencies between the direct and indirect calculation of ΔT . Consequently, we refrain from using such pressure corrections (or from rescaling the parameter κ_2 in the soft mode energy of the effective Hamiltonian, see e.g. Ref. 25) in this work. As a result, our calculated transition temperature T_c for the cubic to tetragonal phase transition (~ 270 K) deviates from the known experimental value (403 K). However, it can be expected that nevertheless trends are accurately described and that the calculated temperature changes (after rescaling for the correct number of degrees of freedom) are also quantitatively of the right magnitude.

Case	Switching on	Switching off
Paraelectric phase ($T > T_c$)		
Instantaneous	0	$\chi \mathcal{E}_{\text{app}}^2$
Ramping	$-\frac{1}{2} \chi \mathcal{E}_{\text{app}}^2$	$\frac{1}{2} \chi \mathcal{E}_{\text{app}}^2$
Ferroelectric phase ($T < T_c$)		
Instantaneous	$-P_0 \mathcal{E}_{\text{app}}$	$P_0 \mathcal{E}_{\text{app}} + \chi' \mathcal{E}_{\text{app}}^2$
Ramping	$-P_0 \mathcal{E}_{\text{app}} - \frac{1}{2} \chi' \mathcal{E}_{\text{app}}^2$	$P_0 \mathcal{E}_{\text{app}} + \frac{1}{2} \chi' \mathcal{E}_{\text{app}}^2$

TABLE I. The changes in the total energy on varying the applied electric field are tabulated for instantaneous switching and slow ramping of the field. “Switching on” corresponds to the field varying from zero to \mathcal{E}_{app} , and vice-versa for the “switching off” case. The formulas are derived using the following simplified assumption: the induced polarization P_{ind} depends linearly on the applied field \mathcal{E} , the proportionality constant is the dielectric susceptibility χ in the paraelectric phase and χ' in the ferroelectric phase. P_0 is the spontaneous polarization of the system in the ferroelectric phase.

III. RESULTS AND DISCUSSION

A. Rate dependence

First, we investigate the influence of the rate of change, $d\mathcal{E}/dt$, with which the electric field is ramped up or down in our simulations. This is an important technical point, since, depending of course on the invested computational resources, MD simulations can only cover time periods of up to a few nano seconds. This means that within the simulations, the electric field needs to be changed extremely fast compared to a real experiment. Nevertheless, it is very important to ensure that the system always stays in thermal equilibrium and that the MD simulation indeed describes a reversible process.

We start by analyzing the change of the total energy under application of an electric field for the two cases of instantaneous electric field switching and very slow ramping. In general, the change in total energy ΔE_{tot} under application or removal of an electric field is given by $\Delta E_{\text{tot}} = -\int P \cdot d\mathcal{E}$, where P is the polarization of the system. For instantaneous switching, the polarization cannot follow the change of the applied field and stays essentially constant during the switching process. In the paraelectric phase, the spontaneous polarization is zero. Therefore, when the field is switched on instantaneously for $T > T_c$, ΔE_{tot} is also equal to zero. However, if the field is instantaneously switched off from some finite value \mathcal{E}_{app} , then even at $T > T_c$, there is an induced polarization, $P_{\text{ind}} = \chi \mathcal{E}_{\text{app}}$, resulting in a non-zero $\Delta E_{\text{tot}} = P_{\text{ind}} \cdot \mathcal{E}_{\text{app}} = \chi \mathcal{E}_{\text{app}}^2$. This implies that the complete cycle of applying and removing an electric field instantaneously to the system results in an irreversible process.

On the other hand, if the field is applied/removed slowly, then the polarization can follow the external field,

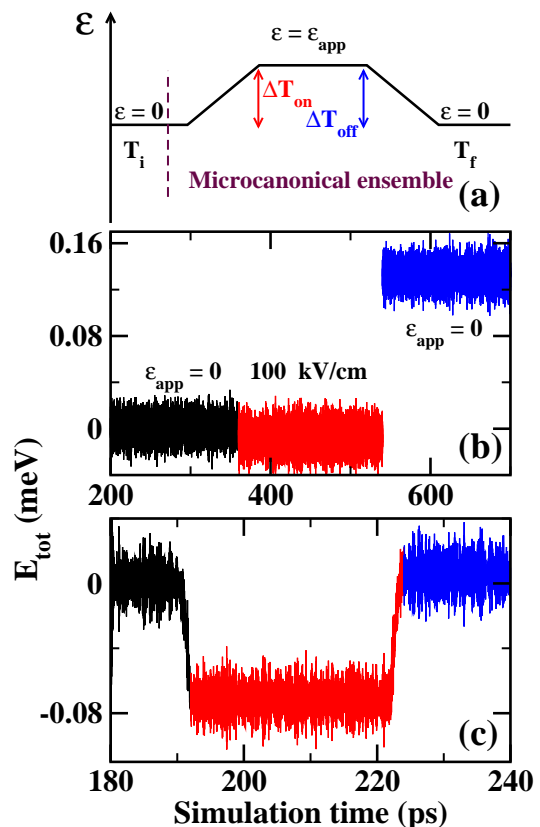


FIG. 1. (Color online) (a) Schematic depiction of the simulation cycle (see text). Panels (b) and (c) show the total energy as a function of MD steps for instantaneous field application/removal and for slow field ramping, respectively. Here, the starting temperature T_i is 530 K and the applied field is 100 kV/cm. In (c) the rate of change of the applied field is equal to $0.05 \text{ kVcm}^{-1}\text{fs}^{-1}$. For clarity, the total energy is plotted only after the system is switched to the microcanonical ensemble.

and at each time $P = \chi \mathcal{E}$. The resulting change in total energy is then given according to $\Delta E_{\text{tot}} = -\int_{\mathcal{E}_i}^{\mathcal{E}_f} P \cdot d\mathcal{E} = \pm \frac{1}{2} \chi \mathcal{E}_{\text{app}}^2$. Here, \mathcal{E}_i and \mathcal{E}_f are the initial and final applied fields, respectively, which are equal to zero and \mathcal{E}_{app} for application of the field, and the other way round for removal. The plus and minus signs then correspond to removal and application of \mathcal{E}_{app} , respectively. Thus, it can be seen that slow ramping results in the same magnitude of the total energy change for switching the field on and off, i.e. one obtains a reversible process. Similar arguments hold true within the ferroelectric phase, with an additional term coming from the spontaneous polarization P_0 . The resulting total energy changes for the various cases are tabulated in Table I.

Next, we perform simulations at different temperatures to examine whether the simple considerations outlined in the preceding paragraphs are consistent with the actual MD simulations for the effective Hamiltonian. We have selected two temperatures, $T = 530 \text{ K}$ (in the paraelectric phase) and $T = 270 \text{ K}$ (in the ferroelectric phase, just

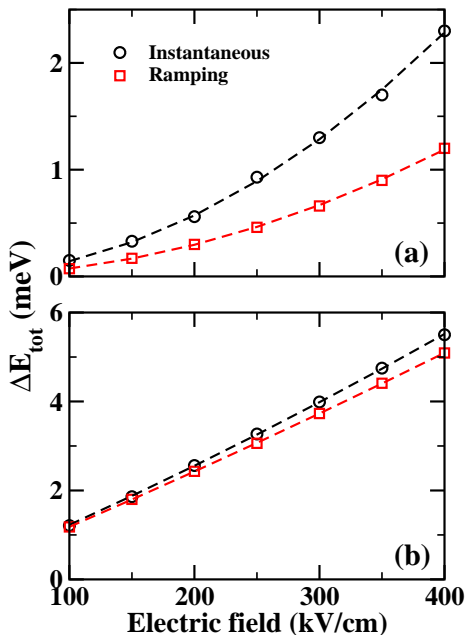


FIG. 2. (Color online) The change in the total energy on switching off the applied field is plotted as a function of applied electric field for (a) the paraelectric phase at $T_i = 530$ K and (b) the ferroelectric phase at $T_i = 270$ K. The rate of change of the applied field $d\mathcal{E}/dt$ is equal to $-0.05 \text{ kVcm}^{-1}\text{fs}^{-1}$ for the “ramping” case (red squares). The symbols show the data points, whereas the dashed lines are fits to the corresponding functional forms listed in Table I.

below the transition temperature), at which we monitor the change in the total energy on switching the field on and then off again for several values of \mathcal{E}_{app} . The full simulation cycle is depicted schematically in Fig. 1(a). First, the system is thermalized at temperature T_i and field $\mathcal{E} = 0$ within the canonical ensemble. The simulation is then switched to the microcanonical ensemble, the electric field is ramped up to \mathcal{E}_{app} , and the resulting temperature change ΔT_{on} is monitored. Then, the field is ramped down again, and the corresponding temperature change ΔT_{off} is monitored. If the system stays in thermal equilibrium during the entire simulation cycle, then both its total energy and its temperature, T_f , at the end of the simulation should be identical to the corresponding starting values, and $\Delta T_{\text{off}} = -\Delta T_{\text{on}}$.

The evolution of the total energy over a full cycle at $T_i = 530$ K, i.e. in the paraelectric phase, is shown in Fig. 1(b). In this simulation, the field is switched instantaneously. As expected, there is no change in the total energy while switching on the field (see Table I), but there is a jump of the total energy when the field is switched off. Fig. 1(c) shows the evolution of the total energy when the field is ramped up and down slowly. In this case, $|\Delta E_{\text{tot}}|$ is the same for application and removal of the field. This confirms that very fast switching of the applied field results in an irreversible process.

Further, we plot the change in the total energy ΔE_{tot}

as a function of the applied field \mathcal{E}_{app} at $T_i = 530$ K and $T_i = 270$ K in Figs. 2(a) and (b), respectively. These ΔE_{tot} values correspond to removal of the field (“switching off”). For slow ramping, these are equal to those obtained from switching on (but with opposite sign). The data from the simulations is fitted using the corresponding functional forms given in Table I. The fits are indicated by dashed lines and match very well with the data. In the paraelectric phase the total energy change for switching off the field depends quadratically on the applied field strength and there is a factor of 2 difference between slow ramping and instantaneous switching. The fit to the instantaneous switching data gives $\chi = 3.5 \times 10^{-2} \mu\text{C} \cdot \text{kV}^{-1}\text{cm}^{-1}$ which matches well with the corresponding value obtained from the ramping data ($\chi = 3.8 \times 10^{-2} \mu\text{C} \cdot \text{kV}^{-1}\text{cm}^{-1}$). In the ferroelectric phase, ΔE_{tot} is dominated by the linear contribution stemming from the spontaneous polarization. From the fit of the instantaneous switching data, we obtain $P_0 = 30.32 \mu\text{C}/\text{cm}^2$ and $\chi' = 1.3 \times 10^{-2} \mu\text{C} \cdot \text{kV}^{-1}\text{cm}^{-1}$, whereas for the case of slow ramping the corresponding quantities are $30.32 \mu\text{C}/\text{cm}^2$ and $1.5 \times 10^{-2} \mu\text{C} \cdot \text{kV}^{-1}\text{cm}^{-1}$ respectively. There is good agreement between these two data sets. Similarly, the value for P_0 obtained from fitting ΔE_{tot} for instantaneous “switching on” of the electric field (not shown here) is equal to $30.31 \mu\text{C}/\text{cm}^2$. We can also compare these values for the spontaneous polarization to that obtained directly from the MD simulations at $T = 270$ K, which is equal to $28.2 \mu\text{C}/\text{cm}^2$. Note that the agreement between the various parameters is excellent considering the simplicity of the approach. This shows that the simple considerations outlined at the beginning of this section do indeed lead to a consistent description of the various switching cases.

Fig. 3(a) shows the obtained temperature changes when the electric field is switched on and off, ΔT_{on} and ΔT_{off} , as function of the inverse rate $(d\mathcal{E}/dt)^{-1}$, with which the field is ramped up and down, for a starting temperature $T_i = 350$ K (i.e. close to the maximum EC effect). Instantaneous switching corresponds to $(d\mathcal{E}/dt)^{-1} = 0$ and slow ramping corresponds to a large inverse rate. It can be seen that for small inverse ramping rates, i.e. for fast switching, $|\Delta T_{\text{on}}| \neq |\Delta T_{\text{off}}|$. The difference between the values is about 9 K which is significant compared to the converged EC temperature change of 17.6 K observed at this temperature.²⁶ This implies that the system goes out of equilibrium during fast switching, consistent with the total energy considerations discussed above. As the rate is reduced (i.e. the inverse rate is increased), the difference between $|\Delta T_{\text{on}}|$ and $|\Delta T_{\text{off}}|$ becomes smaller, and already for an inverse rate of $500 \text{ kV}^{-1}\cdot\text{fs}\cdot\text{cm}$ (corresponding to $|d\mathcal{E}/dt| = 0.002 \text{ kVcm}^{-1}\text{fs}^{-1}$), the difference becomes negligible. Similar behavior can be observed also for other initial temperatures.

In Fig. 3(b), the directly calculated EC temperature change obtained by instantaneously switching off the

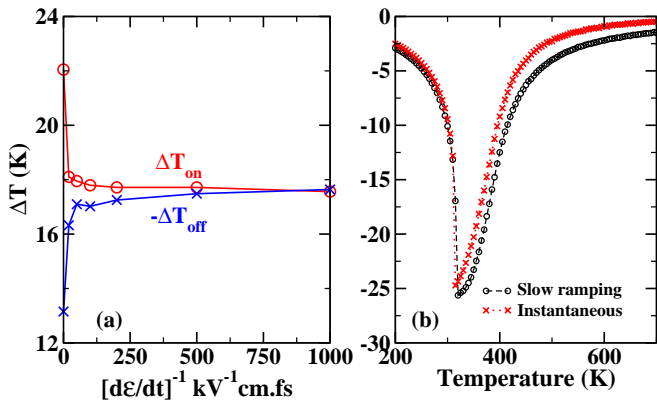


FIG. 3. (Color online) (a) EC temperature changes for switching the electric field on and off, ΔT_{on} and ΔT_{off} , as function of the inverse rate of change of the applied electric field, $(d\mathcal{E}/dt)^{-1}$, for a starting temperature $T_i = 350$ K. The applied field \mathcal{E}_{app} is equal to 200 kV/cm. The simulation cycle used to obtain $\Delta T_{\text{on/off}}$ is depicted in Fig. 1(a). (b) The EC temperature change ΔT as a function of temperature is plotted for slow ramping and instantaneous ramping of the field. The field is varied from 225 kV/cm to 0 kV/cm.

electric field is compared with the one obtained using slow field ramping ($d\mathcal{E}/dt = -0.002$ kV \cdot cm⁻¹fs⁻¹) for an initially applied field of 225 kV/cm. Note that for these calculations the system is thermalized in the canonical ensemble with a nonzero field, which is removed after switching to the microcanonical ensemble. While the overall behavior is the same for both cases, the instantaneous switching underestimates the magnitude of ΔT at essentially all temperatures. This is consistent with our earlier observations in Fig. 3(a). In addition, the temperature for which the largest temperature change occurs is slightly shifted to lower temperatures.

The maximum ΔT , observed at 320 K in Fig. 3(b), is about -25.6 K for slow ramping. After appropriate rescaling for the correct number of degrees of freedom,^{16,26} this corresponds to an EC temperature change of around 5.1 K, which agrees well with earlier reports for similar applied field strengths.^{21,22} After scaling, the difference between ΔT calculated using instantaneous switching and using slow field ramping is approximately 1 K for the given field strength (except very close to the peaks).

Our results up to now thus demonstrate the necessity of ensuring that the system is in thermal equilibrium throughout the whole MD simulation for a correct direct calculation of the adiabatic EC temperature change. In the following we use a rate $d\mathcal{E}/dt = 0.002$ kVcm⁻¹fs⁻¹ for all our direct calculations of the EC temperature change. Even though this rate is very fast compared to actual experimental rates, it is sufficiently slow to avoid irreversibility in the calculation and also allows for reasonable simulation times.

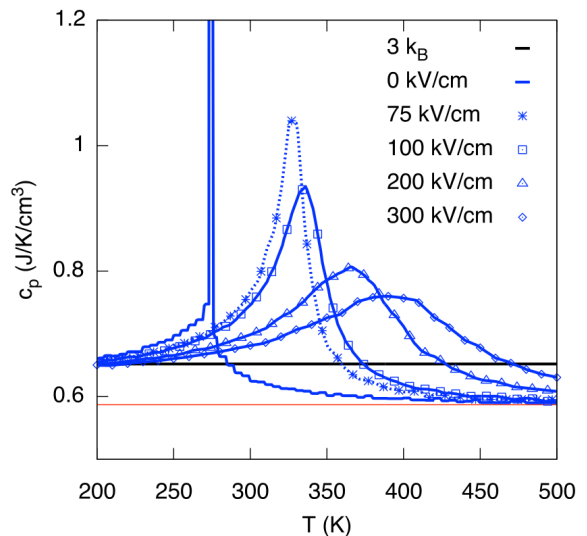


FIG. 4. (Color online) Calculated specific heat of the model Hamiltonian as a function of temperature for different applied electric fields. For better comparison, the Dulong-Petit value of $3 k_B$ is indicated by the thick horizontal black line and the obtained high temperature limit is indicated by the thin horizontal red line.

B. Direct versus indirect EC effect

Next, we compare results from the direct and indirect approaches. As pointed out previously, all calculations are performed using the same effective model Hamiltonian and no experimental data is used. In our previous work, we have calculated the EC effect using the indirect method,^{21,22} but we have used the experimental specific heat value at room temperature to evaluate Eq. (2). Although this is a valid first approximation, this treatment ignores the temperature and electric field dependence of $C_{p,\mathcal{E}}$, as well as the mismatch between the number of degrees of freedom of the real system and the model, which will lead to differences between the results obtained from direct and indirect methods. Therefore, in the present work, we calculate the specific heat from the model Hamiltonian as a function of temperature at different applied fields. This allows for an internally consistent comparison between direct and indirect methods, and also enables us to obtain ΔS^{dir} using the (quasi-) direct method, Eq. (4).

In Fig. 4, we show our results for the specific heat of the effective Hamiltonian as a function of temperature at several applied fields. In absence of an applied field, there is a pronounced peak (divergence) at the ferroelectric transition, which also shows pronounced thermal hysteresis. Such a divergence is characteristic for a first order phase transition. With increasing electric field, the phase transition and thus the peak in the specific heat shift to higher temperature. Furthermore, the transition becomes smoother and the thermal hysteresis disappears for fields of around 25 kV/cm and stronger.

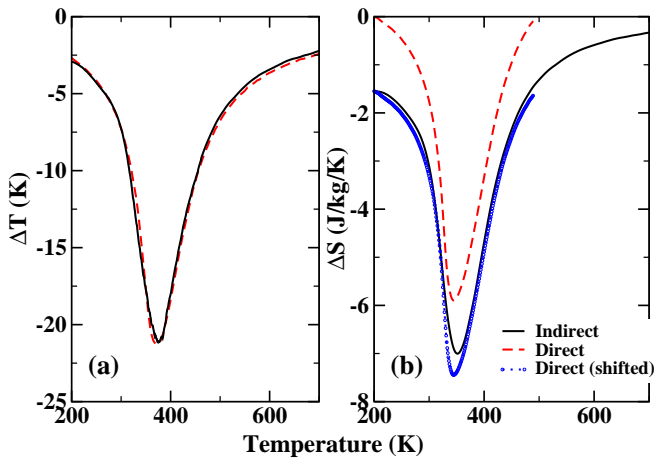


FIG. 5. (Color online) (a) Comparison of the EC temperature change as function of the initial temperature obtained using direct and indirect methods. The field is varied from 300 kV/cm to 75 kV/cm. In the direct calculation slow field ramping with $d\mathcal{E}/dt = -0.002 \text{ kVcm}^{-1}\text{fs}^{-1}$ is used. (b) The EC entropy change as a function of temperature obtained from direct and indirect methods. Here, the applied field is varied from 75 kV/cm to 300 kV/cm. The results of the direct calculations, but with an offset such that it matches the indirect calculation at $T = 200 \text{ K}$ (see text) are indicated by the blue dotted line.

Previous phenomenological thermodynamic calculations and experimental measurements on bulk BaTiO₃ have shown that an applied field of about 10 kV/cm is sufficient to suppress the first order phase transition.^{17,27,28}

Both at high and low temperatures, i.e. away from the phase transition, $C_{p,\mathcal{E}}$ approaches constant values. We recall that our simulations contain only 3 degrees of freedom instead of 15 for the real system. If the Hamiltonian would be exactly quadratic in the 3 soft mode variables, then each degree of freedom would contribute $1k_B$ to the specific heat, and we would expect a value of $3k_B$, which is equal to $0.65 \text{ J}\cdot\text{K}^{-1}\text{cm}^{-3}$, both in the high and low temperature limit. We note that in our purely classical simulations no modes are “frozen in” at low temperatures. We find a high-temperature limit of 0.59 J/K/cm^3 from our calculations. This small discrepancy with the Dulong-Petit value of $3k_B$ results from the higher order terms in the Hamiltonian. These contribute less at low temperatures, and therefore at low temperatures below T_c the calculated value compares well with the Dulong-Petit value.

Next, we compare both the calculated adiabatic EC temperature change ΔT as well as the isothermal EC entropy change ΔS obtained using direct and indirect methods. As mentioned before, we use a rate of $-0.002 \text{ kVcm}^{-1}\text{fs}^{-1}$ for changing the applied field. In Fig. 5(a), we compare the results from direct and indirect calculations of the adiabatic EC temperature change ΔT . These results correspond to removal of the field (“switching off”), i.e. a negative ΔT (as in Fig. 3(b)).

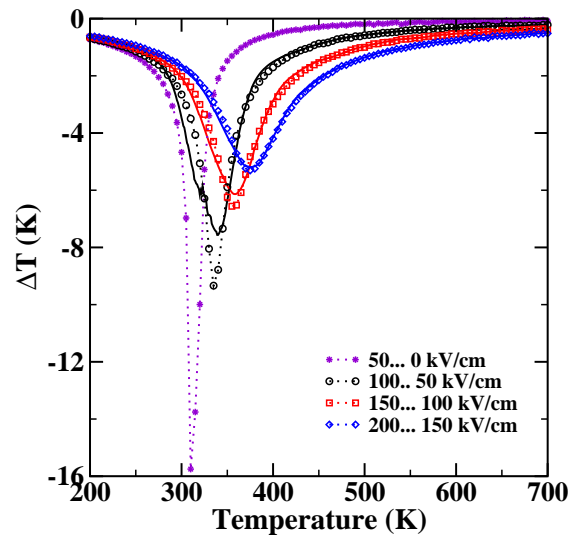


FIG. 6. (Color online) EC temperature change ΔT as function of temperature for different field intervals with the same total width of 50 kV/cm. Results obtained using the direct (indirect) method are shown as dotted lines with symbols (solid lines without symbols).

We consider only fields $\geq 75 \text{ kV/cm}$ for this comparison, in order to exclude the region close to the first order phase transition, where the indirect method is not applicable. It can be seen that the ΔT values calculated from direct and indirect methods match extremely well over the whole temperature range. This shows that within our consistent description, where all quantities are calculated using the same effective Hamiltonian, the direct and indirect approaches indeed lead to exactly the same ΔT . This underlines the validity of the indirect approach to obtain ΔT , which is often preferred in experimental studies, as long as the system does not actually cross the first order phase transition, i.e. for temperatures and electric field strengths above the critical point.^{17,28} We point out, though, that errors can be introduced due to imperfect fits to the statistical measurements, in particular for small fields close to the phase transition, where polarization and specific heat vary strongly. Another source of inaccuracies is the finite sampling of quantities as function of temperature and field, which leads to numerical errors when integrating Eq. (2).

The isothermal entropy change calculated using direct (Eq. (4)) and indirect (Eq. (3)) methods is shown in Fig. 5(b). We note that in principle the specific heat in Eq. (4) is the total specific heat, including electronic, ferroelectric, and all other lattice contributions, while in our treatment using the effective Hamiltonian, only the contributions from the ferroelectric soft mode variables are taken into account. However, since we use exactly the same degrees of freedom to also obtain the temperature- and field-dependent electric polarization for evaluating Eq. (3), we obtain a consistent description within the effective Hamiltonian, and both equations should in prin-

ciple lead to the same value of ΔS . Nevertheless, in contrast to the adiabatic temperature changes, the calculated isothermal entropy changes do not need to be rescaled for the missing degrees of freedom in order to compare with experimental measurements. The entropy change in Eq. (4) depends only on differences in the specific heat for different electric fields, and one can expect, at least to a good approximation, that only the soft mode variables will give significant contributions to this electric field dependence. Consequently, also Eq. (3) does not contain any quantities depending explicitly on the missing degrees of freedom. The effect of the electrons and of other structural degrees of freedom on the temperature and field dependence of the polarization is, to a good approximation, implicitly taken into account by the soft mode variable.

The entropy change shown in Fig. 5(b) corresponds to a change of the electric field from 75 kV/cm to 300 kV/cm, i.e. “switching on”, and therefore a negative ΔS is obtained. Again, we exclude the region of small electric fields close to the phase transition for the comparison of direct and indirect methods. The lower bound for the temperature integration in Eq. (4) is chosen as $T_1 = 200$ K. This temperature is above the second phase transition from the tetragonal ferroelectric to the orthorhombic ferroelectric phase in BaTiO₃ (with the chosen parameterization of the effective Hamiltonian). By definition, the “direct” ΔS calculated from Eq. (4) is zero for $T = T_1$, while the “indirect” ΔS obtained from Eq. (3) has a finite value at $T_1 = 200$ K. Since according to Fig. 4 the calculated specific heat at 200 K shows only negligible field dependence, the finite value of ΔS at this temperature is related to electric-field dependence of the specific heat at lower temperatures, most likely at the two ferroelectric-ferroelectric transitions (tetragonal-orthorhombic and orthorhombic-rhombohedral). For a better comparison between direct and indirect methods we therefore rigidly shift the ΔS curve obtained from the direct method such that it matches the ΔS value obtained from the indirect method at the lowest temperature $T_1 = 200$ K (blue dotted line in Fig. 5). It can be seen that the shifted data agrees quite well with the data obtained from the indirect method. Small deviations can be observed close to the peak at around 350 K, which we ascribe to inaccuracies related to the smoothing/fitting of the specific heat and polarization data and to integration errors due to finite temperature and electric field sampling.

Interestingly, the obtained peak value of $\Delta S \approx 7 \text{ J}\cdot\text{kg}^{-1}\text{K}^{-1}$ is of the same order of magnitude as the maximal value reported for BaTiO₃ single crystals measured in Ref. 29 ($\Delta S = 2.1 \text{ J}\cdot\text{kg}^{-1}\text{K}^{-1}$). However, the corresponding electric field intervals are completely different (75 to 300 kV/cm in our calculations, compared to 0 to 4 kV/cm in Ref. 29), and thus a meaningful quantitative comparison is not easily possible.

Finally, in Fig. 6 we compare the calculated adiabatic

temperature change for different electric field intervals with the same width $|\mathcal{E}_i - \mathcal{E}_f| = 50 \text{ kV/cm}$ but different magnitude of \mathcal{E}_i and \mathcal{E}_f . A first order phase transition occurs only in the electric field interval between $\mathcal{E}_i = 50 \text{ kV/cm}$ and $\mathcal{E}_f = 0 \text{ kV/cm}$. For this interval, we obtain a very narrow peak in ΔT at 310 K, with a maximum value of 15.8 K (corresponding to $\sim 3.2 \text{ K}$ after scaling to the correct N_f). For larger applied fields, the maximum ΔT value shifts to higher temperatures and the corresponding peak broadens.

We note that from our specific heat calculations we can estimate a critical electric field of around 25 kV/cm. For larger fields, the polarization varies continuously with temperature, i.e. no first order phase transition occurs, and the temperature at which $|\partial P/\partial T|_{\mathcal{E}}$ is maximal follows the so-called “Widom line” (see e.g. Refs. 28 and 30). It can be seen that, while the largest ΔT is observed in the field interval containing the first order phase transition (i.e. $\mathcal{E}_i = 50 \text{ kV/cm}$ and $\mathcal{E}_f = 0 \text{ kV/cm}$), the field intervals corresponding to larger $\mathcal{E}_i/\mathcal{E}_f$ also give sizable contributions to the EC effect. We therefore conclude that while the vicinity to the first order transition is important to obtain large changes of polarization with temperature and electric field, and thus large EC effect, the contribution of the transition itself is not essential to obtain large EC response. We note that similar conclusions have been reached in Ref. 30, based on MD simulations for LiNbO₃.

Further, a comparison between ΔT obtained using the direct and indirect methods for the different field intervals again shows a very good agreement for the field intervals corresponding to larger magnitude of \mathcal{E}_i and \mathcal{E}_f , where the variation with temperature and electric field is less strong. Clear discrepancies can be seen for the interval between 100 and 50 kV/cm, where ΔT is rather sharply peaked. These discrepancies result from imperfect smoothing/fitting as well as from numerical integration errors, as already discussed above.

IV. SUMMARY AND CONCLUSIONS

In summary, we have presented a computational study of the EC effect in BaTiO₃ using MD for a first principles-based effective Hamiltonian. We have compared the EC temperature change calculated using direct and indirect methods for bulk BaTiO₃, thereby paying particular attention to the internal consistency of the method. In particular, the temperature and electric field-dependent specific heat has been calculated within the same framework as the temperature- and field-dependent electric polarization (required for the indirect determinations of ΔT), and the same framework has also been used for the direct calculation of ΔT using microcanonical MD.

We have demonstrated that the direct and indirect determination of the adiabatic temperature change leads to identical results provided that the field and temperature region very close to the first order transition, where

the indirect method is not applicable, is excluded. We note that the applicability of Maxwell's relation, Eq. (1), which underlies the indirect determination of the EC temperature change, has been critically discussed for systems close to a first order phase transition (see e.g. the discussion in Refs. 3, 6, and 7). Our results clearly demonstrate the validity of this relation as long as the first order transition is not crossed. Directly at the first order transition, the specific heat diverges and $\partial P/\partial T$ is not defined, and thus the indirect method is not applicable. Very close to the transition, errors can arise due to inaccurate fits, the use of a temperature- and field-independent specific heat, and due to finite temperature and field sampling of the integral in Eq. (2).

Furthermore, we have demonstrated the importance of maintaining thermal equilibrium during the MD simulations for the direct calculation for ΔT , and we have shown that in the present case a ramping rate for the electric field of 0.002 kV/cm/fs is sufficiently slow to ensure reversibility. We note, however, that, due to the neglect of the less important degrees of freedom in the effective Hamiltonian, this is not necessarily representative for the intrinsic relaxation time of BaTiO₃.

In addition, we have (to the best of our knowledge for the first time) used the effective Hamiltonian approach to calculate the isothermal EC entropy change. Similarly to the case of the adiabatic temperature change, we have found good agreement between (quasi-) direct, i.e. via the specific heat, and indirect determination of ΔS . While our calculated values are quantitatively of similar magnitude as available experimental data, further studies for different electric field strengths, possibly also considering the contribution stemming from the latent heat of the first order phase transition, are necessary to obtain a more quantitative comparison between calculated and measured data.

The observation that the largest EC temperature

change occurs in the field interval containing the first order ferroelectric transition ($\mathcal{E}_i = 50$ kV/cm and $\mathcal{E}_f = 0$ kV/cm, see Fig. 6) is in agreement to the giant caloric temperature changes found at other coupled ferroic-structural transitions, e.g. in magnetic Heusler alloys.^{3,31,32} In all these cases, small external fields are able to induce large adiabatic temperature changes, which, however, are restricted to only a narrow temperature interval. Unfortunately, in many cases the thermal hysteresis of the transition leads to a significant reduction of the achievable reversible temperature changes under cycling of the fields, see e.g. Ref. 32. In this respect, the EC effect in BaTiO₃, with its rather low critical field strength, has an important advantage for cooling applications compared to the well-established magnetocaloric Heusler alloys. Beyond the critical field strength, the thermal hysteresis vanishes, leading to a fully reversible EC effect (see also the experimental results in Ref. 33). Furthermore, the transition itself is not crucial for obtaining a large caloric response, as field intervals corresponding to larger $\mathcal{E}_i/\mathcal{E}_f$, i.e. above the critical field strength, also give sizable contributions to the EC effect, see Fig. 6. This is accompanied by a broadening of the ΔT peak with temperature, which is also advantageous for applications. In contrast, the strong first order character of the magneto-structural phase transition in magnetic Heusler alloys is conserved even for giant fields up to 40 T, without a reduction of the thermal hysteresis.³⁴

V. ACKNOWLEDGMENTS

This work was supported by the Swiss National Science Foundation and the German Science Foundation under the priority program SPP 1599 ("Ferroic cooling"). AG thanks the CCSS at the University of Duisburg-Essen for computing time. The work of TN was supported in part by JSPS KAKENHI Grant Number 25400314.

* madhura.marathe@mat.ethz.ch

† claude.ederer@mat.ethz.ch

¹ S. Fähler, U. K. Rössler, O. Kastner, J. Eckert, G. Eggeler, H. Emmerich, P. Entel, S. Müller, E. Quandt, and K. Albe, *Advanced Engineering Materials* **14**, 10 (2011).

² L. Mañosa, A. Planes, and M. Acet, *Journal of Materials Chemistry A* **1**, 4925 (2013).

³ X. Moya, S. Kar-Narayan, and N. D. Mathur, *Nature Materials* **13**, 439 (2014).

⁴ A. S. Mischenko, Q. Zhang, J. F. Scott, R. W. Whatmore, and N. D. Mathur, *Science* **311**, 1270 (2006).

⁵ J. Scott, *Annual Review of Materials Research* **41**, 229 (2011).

⁶ M. Valant, *Progress in Materials Science* **57**, 980 (2012).

⁷ T. Correia and Q. Zhang, eds., *Electrocaloric materials* (Springer, Berlin, 2014).

⁸ S. G. Lu, B. Rožič, Q. M. Zhang, Z. Kutnjak, R. Pirc, M. Lin, X. Li, and L. Gorny, *Applied Physics Letters* **97**, 202901 (2010).

⁹ S. G. Lu, B. Roi, Q. M. Zhang, Z. Kutnjak, and B. Neese, *Applied Physics Letters* **98**, 122906 (2011).

¹⁰ R. Niemann, O. Heczko, L. Schultz, and S. Fähler, *International Journal of Refrigeration* **37**, 281 (2014).

¹¹ Y. Bai, K. Ding, G.-P. Zheng, S.-Q. Shi, and L. Qiao, *Physica Status Solidi A* **209**, 941 (2012).

¹² W. Zhong, D. Vanderbilt, and K. M. Rabe, *Physical Review Letters* **73**, 1861 (1994).

¹³ W. Zhong, D. Vanderbilt, and K. M. Rabe, *Physical Review B* **52**, 6301 (1995).

¹⁴ T. Nishimatsu, U. V. Waghmare, Y. Kawazoe, and D. Vanderbilt, *Physical Review B* **78**, 104104 (2008).

¹⁵ I. Ponomareva and S. Lisenkov, *Physical Review Letters* **108**, 167604 (2012).

¹⁶ T. Nishimatsu, J. A. Barr, and S. P. Beckman, *Journal of the Physical Society of Japan* **82**, 114605 (2013).

¹⁷ N. Novak, Z. Kutnjak, and R. Pirc, *EPL* **103**, 47001 (2013).

- ¹⁸ T. Nishimatsu, M. Iwamoto, Y. Kawazoe, and U. V. Waghmare, *Physical Review B* **82**, 134106 (2010).
- ¹⁹ S. Prosandeev, I. Ponomareva, and L. Bellaiche, *Physical Review B* **78**, 052103 (2008).
- ²⁰ S. Lisenkov and I. Ponomareva, *Physical Review B* **80**, 140102 (2009).
- ²¹ S. Beckman, L. Wan, J. A. Barr, and T. Nishimatsu, *Materials Letters* **89**, 254 (2012).
- ²² M. Marathe and C. Ederer, *Applied Physics Letters* **104**, 212902 (2014).
- ²³ Z. Wu and R. Cohen, *Physical Review B* **73**, 235116 (2006).
- ²⁴ S. D. Bond, B. J. Leimkuhler, and B. B. Laird, *Journal of Computational Physics* **151**, 114 (1999).
- ²⁵ L. Walizer, S. Lisenkov, and L. Bellaiche, *Physical Review B* **73**, 144105 (2006).
- ²⁶ As pointed out in Sec. II, the directly calculated temperature change shown in Figs. 3 and 5 is overestimated compared to the real system, since only 3 dynamic degrees of freedom are included in the effective Hamiltonian (compared to 15 degrees of freedom in the real system). Thus, the overestimation is approximately by a factor of 5, if one assumes that for the real as well as for the model system each degree of freedom contributes equally at all temperatures (see e.g. Ref. 16).
- ²⁷ J. Zhang, A. A. Heitmann, S. P. Alpay, and G. A. Rossetti, Jr., *Journal of Materials Science* **44**, 5263 (2009).
- ²⁸ N. Novak, R. Pirc, and Z. Kutnjak, *Physical Review B* **87**, 104102 (2013).
- ²⁹ X. Moya, E. Stern-Toulats, S. Crossley, D. González-Alonso, S. Kar-Narayan, A. Planes, L. Mañosa, and N. D. Mathur, *Advanced Materials* **25**, 1360 (2013).
- ³⁰ M. C. Rose and R. E. Cohen, *Physical Review Letters* **109**, 187604 (2012).
- ³¹ A. Planes, M. Mañosa, and M. Acet, *Journal of Physics: Condensed Matter* **21**, 233201 (2009).
- ³² J. Liu, T. Gottschall, K. P. Skokov, J. D. Moore, and O. Gutfleisch, *Nature Materials* **11**, 620 (2012).
- ³³ S. Kar-Narayan and N. D. Mathur, *Journal of Physics D: Applied Physics* **43**, 032002 (2010).
- ³⁴ C. S. Mejía, M. G. Zavareh, A. K. Nayak, Y. Skourski, J. Wosnitza, C. Felser, and M. Nicklas, *Journal of Applied Physics* **117**, 17E710 (2015).